Available online at www.sciencedirect.com
SCIENCE DIRECT®
Chemical Physics Letters 404 (2005) 85–89
CHEMICAL PHYSICS LETTERS
www.elsevier.com/locate/cplett

Highly ^{13}C isotope enriched azafullerene, $C_{59}N$, for nuclear spin labelling

F. Simon [a,*], F. Fülöp [b], A. Rockenbauer [b,c], L. Korecz [b,c], H. Kuzmany [a]

[a] Institut für Materialphysik, Universität Wien, Strudlhofgasse 4, AT-1090 Wien, Austria
[b] Budapest University of Technology and Economics, Institute of Physics and Solids in Magnetic Fields Research Group of the Hungarian Academy of Sciences, H-1521, Budapest, P.O. Box 91, Hungary
[c] Chemical Research Center of the Hungarian Academy of Sciences, P.O. Box 17, Budapest H-1525, Hungary

Received 17 November 2004; in final form 3 January 2005

Abstract

Synthesis of highly ^{13}C isotope enriched azafullerene, $C_{59}N$ embedded in C_{60} is reported. ^{13}C enriched fullerenes, produced with the Krätschmer–Huffmann process, were subject to a N_2 discharge that produces $C_{59}N$ with a low probability. Raman spectroscopy indicates a homogeneous ^{13}C distribution. Electron spin resonance measurement (ESR) proves that the $C_{59}N$ concentration, 0.2%, is similar as in non-enriched fullerenes. The ESR spectrum is simulated accurately with the known ^{14}N and ^{13}C hyperfine coupling constants. The material enables the nuclear spin-labelling of heterofullerene complexes with a potential for biological applications. It might also find applications as a building element for quantum computation.

1. Introduction

Isotope controlled synthesis (ICS) of molecular nanostructures provides an important degree of freedom to characterize fundamental and application oriented properties. ICS is generally considered as a tool to, e.g., enhance nuclear magnetic resonance signals, to provide improved information when specific isotope labelling is possible or to trace biological processes using radioactive nuclei. For fullerenes [1], ICS was applied to improve the NMR data [2], to identify the origin of different vibrational modes in crystalline C_{60} [3], and to yield an insight into underlying physical phenomenon such as the mechanism of the superconductivity in alkali doped fullerides [4] by means of ^{13}C enrichment. More recently, ^{13}C enriched fullerenes were used to produce ^{13}C enriched single wall carbon nanotubes [5].

Properties of fullerenes can be also studied through the synthesis of on-ball doped modifications. The $C_{59}N$ or $C_{59}B$ heterofullerenes were predicted to provide a doping opportunity for C_{60} [6,7]. In general, heterofullerenes possess a rich chemistry due to their enhanced reactivity as compared to pristine fullerenes [7]. The $C_{59}N$ azafullerene can be synthesized in macroscopic amounts [7,8] and in a solid form it is an insulator consisting of $(C_{59}N)_2$ dimer units where the extra electrons are localized in the dimer bonds as singlet states [9]. The $C_{59}N$ monomer radical can be observed by light [10,11] or thermal induced homolysis of $(C_{59}N)_2$ [12] or when the $C_{59}N$ monomer is embedded in a low concentration in the C_{60} crystal [13]. This $C_{59}N$:C_{60} solid solution was synthesized in a discharge tube designed for the production of $N@C_{60}$ [13]. The advantages of the latter synthesis method over the chemical synthesis [8] are its relative simplicity and the ability of providing an isotope control option by changing the $^{14}N_2$ gas to $^{15}N_2$. Recently, it was shown that the extra electron on the $C_{59}N$ is transferred toward the C_{60}'s at high

* Corresponding author. Fax: +43 1 4277 51375.
E-mail address: fsimon@ap.univie.ac.at (F. Simon).

0009-2614/$ - see front matter © 2005 Elsevier B.V. All rights reserved.
doi:10.1016/j.cplett.2005.01.056

temperatures and it provides a controllable electron doping of the crystalline C_{60} [14].

Here, we report the synthesis of the $C_{59}N$ monomer radical with controlled ^{13}C isotope content. The material was prepared from C_{60} containing isotopically controlled amounts of ^{13}C using the N_2 discharge method. Raman spectroscopy indicates a uniform ^{13}C enrichment of the fullerenes. The ^{13}C enriched $C_{59}N$:C_{60} material was studied with electron spin resonance. The ^{14}N hyperfine triplet, that dominates the spectrum for non-isotope enriched $C_{59}N$:C_{60}, collapses into a broad line in agreement with the isotope content and the ^{13}C nuclear hyperfine couplings determined previously in $C_{59}N$ [13]. A minority phase that is poor in ^{13}C was also observed underlying the sensitivity of the ESR method in characterizing this material.

2. Experimental

2.1. Sample preparation

Commercial ^{13}C isotope enriched fullerene mixture (MER Corp., Tucson, USA) was used for the synthesis of $C_{59}N$. The isotope enriched fullerenes were produced by the Krätschmer–Huffmann process [15] using ^{13}C enriched graphite rods. The supplier provided a ^{13}C enrichment of nominal 25% that was determined using mass spectrometry. The isotope enriched fullerenes are denoted as $(^{13}C_x)_{60}$ and $(^{13}C_x)_{59}N$ in the following. We refer to the material with the nominal $x = 0.25$ ^{13}C content, although this value is slightly refined in this work. Apart from the C_{70} and other higher fullerenes with contents up to 20%, the dominant impurity in the material is a $(^{13}C_x)_{60}$ phase with $x \approx 0.05$ and a content below 2%. The high purity C_{60} (>99.9%) used for comparison was obtained from Hoechst (Hoechst AG, Frankfurt, Germany). $C_{59}N$ production was performed in the same N_2 discharge tube as previously [13] following the original design of Pietzak et al. [16] for the production of N@C_{60}:C_{60}. In brief, fullerenes are sublimed into a nitrogen discharge that is maintained by a high voltage between two electrodes inside a quartz tube filled with a low pressure of N_2 gas. $C_{59}N$:C_{60} deposits on surfaces with temperatures between 200 and 400 °C of the quartz tube, whereas N@C_{60}:C_{60} deposits on the water-cooled cathode. The resulting material is collected from the tube walls and is resublimed at 500 °C twice in order to remove impurities that are usually produced during the synthesis and to reduce the amount of higher fullerenes [17]. However, the less ^{13}C enriched C_{60} phase can not be removed from the sample with this method. Typically 10 mg of final material containing $(^{13}C_{0.25})_{59}N$ at 2000 ppm concentrations in $(^{13}C_{0.25})_{60}$ is produced from 100 mg starting fullerene material. The samples were sealed in quartz tubes under vacuum for the ESR and Raman measurements. Among the higher fullerenes, C_{70} can be best observed using Raman spectroscopy and its amount was found to be below 1% in the final material.

2.2. Raman spectroscopy

Multi frequency Raman spectroscopy was studied on a Dilor xy triple spectrometer at 488 nm excitation energy using an Ar–Kr mixed-gas laser.

2.3. Electron spin resonance spectroscopy

The ESR experiments were performed with a Bruker Elexsys X-band spectrometer. A typical microwave power of 1 mW and 0.01 mT magnetic field modulation at ambient temperature were used.

3. Results and discussion

In Fig. 1, we show the Raman spectra of $(^{13}C_{0.25})_{59}N$:$(^{13}C_{0.25})_{60}$ and C_{60} with natural carbon isotope contents at ambient conditions and excited with a 488 nm laser. The spectrum of $(^{13}C_{0.25})_{59}N$:$(^{13}C_{0.25})_{60}$ is identical to that of $(^{13}C_{0.25})_{60}$ as the Raman technique is not sensitive to the 2000 ppm amounts of $(^{13}C_{0.25})_{59}N$. We focus our attention on the totally symmetric $A_g(2)$ mode that appears with the largest intensity for this laser excitation [17]. Analysis of this mode enables us to determine the ^{13}C enrichment level with precision and

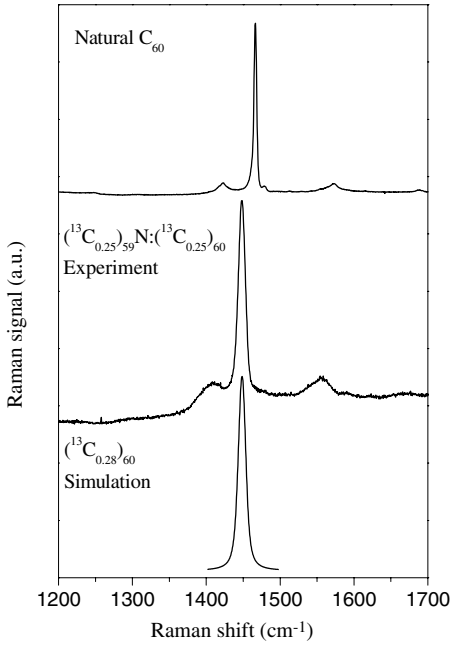

Fig. 1. Raman spectra of natural C_{60} and $(^{13}C_{0.25})_{59}N$:$(^{13}C_{0.25})_{60}$ at $\lambda = 488$ nm excitation. The lowest solid curve show the simulated C_{60} $A_g(2)$ mode with 28% ^{13}C enrichment as explained in the text.

provides information on its homogeneity. A similar analysis was performed previously [18,19]. As the ^{13}C build-in in the C_{60}'s is a random process, the number of ^{13}C nuclei on a given $(^{13}C_x)_{60}$ fullerene is expected to follow a binomial distribution with $x \cdot 60$ expectation value. The vibrational frequency of the ^{13}C enriched fullerenes downshifts as a result of the heavier ^{13}C. In a continuum approximation the amount of the downshift is given by: $(v_0 - v)/v_0 = 1 - \sqrt{\frac{12+c_0}{12+c}}$, where v_0 and v are the Raman shifts of the corresponding modes in the natural carbon and enriched materials, respectively, c is the concentration of the ^{13}C enrichment, and $c_0 = 0.011$ is the natural abundance of ^{13}C in carbon. The experimentally observed 16.0(5) cm^{-1} downshift of the first moment of the $A_g(2)$ mode, corresponds to $c = 0.28(1)$. In addition, the full line-shape was simulated from the convolution of the binomial distribution with the line-shape of this mode in the natural C_{60}. A good agreement between the experimentally observed line-shape and the simulation (lowest solid curve in Fig. 1) was obtained using the above value for c. This proves that the distribution of the ^{13}C nuclei follows the statistical expectation and is therefore homogeneous. The current $c = 0.28(1)$ is slightly different from the value, $c = 0.25$, given by the supplier underlining the difficulty of the ^{13}C content determination.

In order to further characterize the material, we compared its Raman spectra with that of the starting fullerene mixture (not shown). The absence of the C_{70} peaks puts a 2% upper limit on the total amount of residual higher fullerenes in our material as compared to the starting value of about 20%. This proves that the double sublimation procedure at 500 °C is indeed very effective in purifying the material from higher fullerenes. The $(^{13}C_x)_{60}$ phase with $x \approx 0.05$ that was observed with mass spectroscopy by the supplier is not removed by the double sublimation, however its content is below the detectability limit. In contrast, electron spin resonance spectroscopy can detect the fraction of the sample that belongs to the different $(^{13}C_x)_{59}N$ radicals.

In Fig. 2, we show the room temperature ESR spectrum of the $(^{13}C_{0.25})_{59}N$:$(^{13}C_{0.25})_{60}$ material with two different magnetic field scales. We also show the spectrum of non-enriched $C_{59}N$:C_{60} for comparison. The spectra of the latter was analyzed in detail previously [13] and is recalled here. The dominating triplet component was identified as due to the ^{14}N ($I = 1$) hyperfine interaction. The free tumbling of the molecule above the *sc-fcc* structural transition of the C_{60}, $T_c = 261$ K [17], averages out the anisotropic part of this hyperfine coupling. However, the electron is delocalized on the $C_{59}N$ cage and a number of well defined ^{13}C ($I = 1/2$) satellite doublets appear as a result of the finite electron density on the different C positions and the 1.1% abundance of ^{13}C in

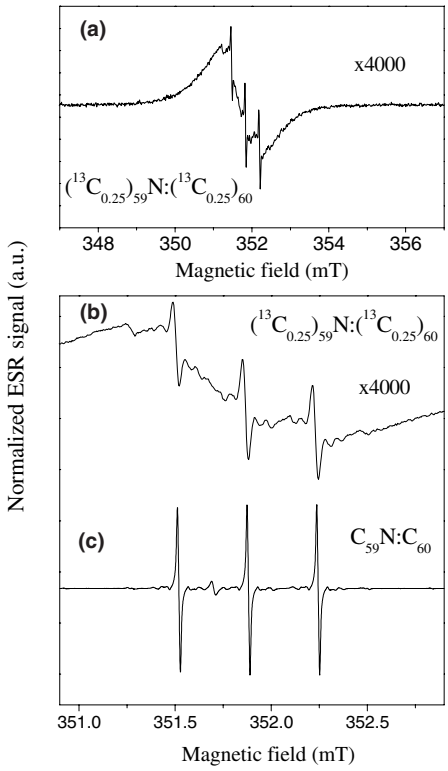

Fig. 2. ESR spectra of $C_{59}N$:C_{60} produced from (a–b) ^{13}C enriched and (c) natural carbon normalized by the sample mass. Note the different field scales for (a) and (b–c) and the enlarged scaling for the enriched materials.

carbon. The hyperfine couplings were determined for eight non-equivalent carbon sites corresponding to 23 sites on the $C_{59}N$ molecule. An additional small intensity signal between the two low-field ^{14}N triplet lines was identified as a $C_{59}N^+$–C_{60}^- heterodimer due to a partial charge transfer from $C_{59}N$ [14].

The $(^{13}C_x)_{59}N$ spectrum is simulated for arbitrary x by using a recursive build-up technique [20]. The effect of the first ^{13}C coupling is computed by superimposing a doublet pattern with intensity x onto each components of the original nitrogen triplet signal with intensity of $1 - x$. In the next step, this superimposed spectrum is considered as a starting signal and the next superimposition is carried out in the same way by using the next carbon splitting constant. The new carbon splitting could have the same value as the preceding one in the case of equivalent carbons. The procedure is repeated for all the 23 carbon nuclei with resolved splitting. The impact of the 36 non-resolved carbon splittings can be considered by using an increased intrinsic line-width in the primer spectrum. Similarly, the small intensity $C_{59}N^+$–C_{60}^- heterodimer signal becomes unobservable due to its broadening.

The ESR spectrum of the $(^{13}C_{0.25})_{59}N$:$(^{13}C_{0.25})_{60}$ consists of apparently two overlapping signals: a broad component and a triplet signal together with a ^{13}C

hyperfine pattern. The ^{13}C hyperfine structure is similar to that observed in the non-enriched $C_{59}N$, however its components have an increased line-width that results from the hyperfine interaction of the non-resolved C sites. The double integrated and mass normalized intensities, that measures the number of spins in the sample, are similar for the natural and enriched materials suggesting that the complicated pattern in the enriched sample also originates from the $C_{59}N$ radicals, however, the presence of ^{13}C broadens its spectrum. Below, we show that the observed ESR pattern reflects the inhomogeneity in our sample. The narrow triplet and the broader components originate from the less and highly ^{13}C enriched phases, respectively.

In Fig. 3a, we show the experimental spectrum again together with a simulation for a sample containing a mixture of $(^{13}C_x)_{59}N$ molecules with $x = 0.28$ and $x = 0.045$ enrichments (Fig. 3b) with intensity ratios of 98.2:1.8, respectively. The g-factors of the two components were taken to be identical with that of the non-enriched $C_{59}N$ of $g = 2.0014(2)$. A residual 0.04 mT line-width was assumed to account for the hyperfine interactions of the non-resolved C sites. The combination of these spectra was found to simulate best the experimental curve. It was assumed that the molecules are freely rotating and the spectra can be described using the previously determined hyperfine coupling constants. The simulated spectra are shown separately for the two types of molecules in Fig. 3c and d, respectively. Although, the two kinds of molecules have a similar ESR amplitude, they have very different integrated intensities. We recall that the ESR signal intensity is inversely proportional to the square of the linewidth due to the field modulation technique employed. As a result, the narrow structure is only a tiny, <2% fraction of the total ESR signal intensity. This small amount of ^{13}C poorer phase is an unwanted side-product of the production of the higher ^{13}C enriched material, however, its amount may not be a limiting factor for practical applications.

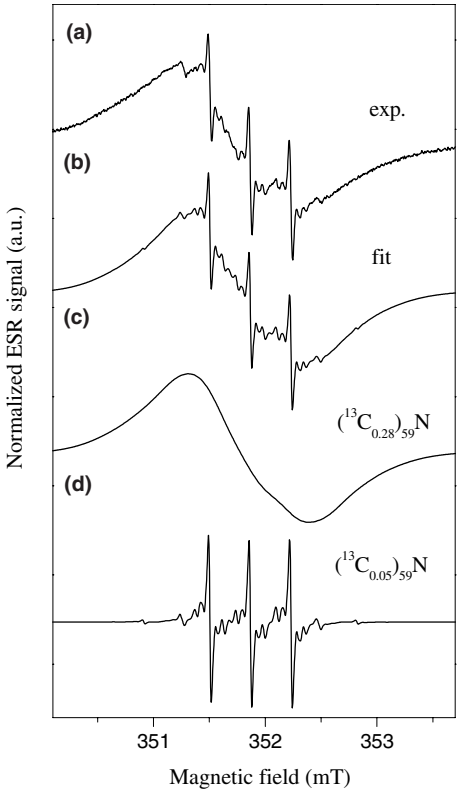

Fig. 3. Comparison of the experimental ESR spectra of $(^{13}C_{0.25})_{59}N$:$(^{13}C_{0.25})_{60}$ (a) with the simulation as explained in the text (b). Simulated spectra for the two levels of isotope enrichments, $(^{13}C_{0.28})_{59}N$:$(^{13}C_{0.25})_{60}$ (c) and $(^{13}C_{0.05})_{59}N$:$(^{13}C_{0.25})_{60}$ (d) are also shown.

4. Conclusion

In conclusion, we presented the preparation of a ^{13}C enriched heterofullerene, the $^{13}C_{59}N$ azafullerene, from ^{13}C enriched fullerenes. Raman and ESR spectroscopy was used to characterize the enrichment and its homogeneity. The material was produced in a nitrogen discharge tube with the same yield as the non-enriched material. This synthesis method opens new prospects for applications of the chemically active heterofullerenes. These include nuclear spin-labelling of bio-molecules with heterofullerenes or the nuclear spin labelling of the biologically active fullerene itself such as in the HIV-1 inhibitor fullerene derivatives [21]. In addition, an emerging field where application of the current system is envisaged is the use of molecules with well defined interaction configurations between electron and nuclear spins for the purpose of quantum computing [22–24].

Acknowledgements

The authors gratefully acknowledge stimulating discussions with A. Jánossy. This work was supported by the Austrian Science Funds (FWF) Project No. 17365, by the EU Project NANOTEMP BIN2-2001-00580, PATONN MEIF-CT-2003-501099 and the Hungarian State Grants OTKA TS040878, OTKA NDF45172, OTKA T043255 and T046953. FS acknowledges the Bolyai Hungarian Research Fellowship.

References

[1] H.W. Kroto, J.R. Heath, S.C. O'Brien, R.F. Curl, R.E. Smalley, Nature 318 (1985) 162.
[2] For a review see: C.H. Pennington, V.A. Stenger, Rev. Mod. Phys. 68 (1996) 885.
[3] M.C. Martin, J. Fabian, J. Godard, P. Bernier, J.M. Lambert, L. Mihály, Phys. Rev. B 51 (1995) 2844.

[4] For a review see: O. Gunnarsson, Rev. Mod. Phys. 69 (1997) 575, and Alkali-doped Fullerides. Narrow-band Solids with Unusual Properties, World Scientific, Singapore, 2004.
[5] F. Simon, Ch. Kramberger, R. Pfeiffer, H. Kuzmany, V. Zolyomi, J. Kurti, P.M. Singer, H. Alloul, cond-mat/0406343.
[6] W. Andreoni, F. Gygi, M. Parrinello, Chem. Phys. Lett. 190 (1992) 159.
[7] J.C. Hummelen, C. Bellavia-Lund, F. WudlHeterofullerenes in Topics in Current Chemistry, vol. 199, Springer, Berlin, Heidelberg, 1999, p. 93.
[8] J.C. Hummelen, B. Knight, J. Pavlovich, R. Gonzalez, F. Wudl, Science 269 (1995) 1554.
[9] T. Pichler, M. Knupfer, M.S. Golden, S. Haffner, R. Friedlein, J. Fink, W. Andreoni, A. Curioni, M. Keshavarz-K, C. Bellavia-Lund, A. Sastre, J.-C. Hummelen, F. Wudl, Phys. Rev. Lett. 79 (1997) 3026.
[10] A. Gruss, K.-P. Dinse, A. Hirsch, B. Nuber, U. Reuther, J. Am. Chem. Soc. 119 (1997) 8728.
[11] K. Hasharoni, c. Bellavia-Lund, M. Keshavarz-K, G. Srdanov, F. Wudl, J. Am. Chem. Soc. 119 (1997) 11128.
[12] F. Simon, D. Arčon, N. Tagmatarchis, S. Garaj, L. Forró, K. Prassides, J. Phys. Chem. A. 103 (1999) 6969.
[13] F. Fülöp, A. Rockenbauer, F. Simon, S. Pekker, L. Korecz, S. Garaj, A. Jánossy, Chem. Phys. Lett. 334 (2001) 233.
[14] A. Rockenbauer, et al., unpublished.
[15] W. Krätschmer, L.D. Lamb, K. Fostiropoulos, D.R. Huffmann, Nature 347 (1990) 354.
[16] B. Pietzak, M. Waiblinger, T.A. Murphy, A. Weidinger, M. Hohne, E. Dietel, A. Hirsch, Chem. Phys. Lett. 279 (1997) 259.
[17] M.S. Dresselhaus, G. Dresselhaus, P.C. Ecklund, Science of Fullerenes and Carbon Nanotubes, Academic Press, 1996.
[18] A. Rosenberg, C. Kendziora, Phys. Rev. B 51 (1995) 9321.
[19] P.J. Horoyski, M.L.W. Thewalt, T.R. Anthony, Phys. Rev. B 54 (1996) 920.
[20] A. Rockenbauer, L. Korecz, Appl. Magn. Reson. 10 (1996) 29.
[21] S.H. Friedman, D.L. DeCamp, R.P. Sijbesma, G. Srdanov, F. Wudl, G.L. Kenyon, J. Am. Chem. Soc. 115 (1993) 6506.
[22] W. Harneit, C. Meyer, A. Weidinger, D. Suter, J. Twamley, Phys. Stat. Sol. B 233 (2002) 453.
[23] M. Mehring, J. Mende, W. Scherer, Phys. Rev. Lett. 90 (2003) 153001.
[24] W. Scherer, A. Weidinger, M. Mehring, in: H. Kuzmany, J. Fink, M. Mehring, S. Roth (Eds.), Electronic Properties of Synthetic Nanostructures, AIP Conference Proceedings, New York, 2004, p. 315.